International Journal of Mechanical, Industrial and Aerospace Sciences
ISSN: 2517-9950
Vol:7, No:6, 2013

Effect of Impact Location upon Sub-Impacts between Beam and Block

T. F. Jin, X. C. Yin, and P. B. Qian

***Abstract*—**The present investigation is concerned with sub-impacts taken placed when a rigid hemispherical-head block transversely impacts against a beam at different locations. Dynamic substructure technique for elastic-plastic impact is applied to solve numerically this problem. The time history of impact force and energy exchange between block and beam are obtained. The process of sub-impacts is analyzed from the energy exchange point of view. The results verify the influences of the impact location on impact duration, the first sub-impact and energy exchange between the beam and the block.

***Keywords*—**Beam, sub-impact, substructure, elastic-plasticity.

I. Introduction

IMPACT event generally includes sub-impacts [1]. To the authors' best knowledge, the existence of sub-impacts was first guessed by Mason [2], who indicated that an impact event which appeared single to the naked eye consisted of several collisions in quick succession. Goldsmith [3] mentioned the phenomenon of sub-impacts, so called multi-impacts in his monograph, and remarked that sub-impact was a peculiar characteristic of impacts involving flexible systems.

Due to short duration of sub-impacts, it was not easy to be captured. Stoianovici and Hurmuzlu [1] applied a high speed video system to record the kinematic data of hardened steel bars dropping on a massive cast iron block with low impact velocity, and observed the occurrence of sub-impacts, which validated Mason's guess.

There were an increasing number of papers concerned with sub-impacts in the past years. Yin [4] investigated the impact problem of two concentric, hollow, circular, elastic cylinders of same materials with zero clearance. The influence of sub-collisions and sub-separations on interface impact pressures, dynamic radial displacements and stresses, was considered. Marur [5] observed double sub-impacts in Charpy impact test, and the interval between the two sub-impacts was as short as one millisecond. Yin and Wang [6] studied the effect of sub-impacts on the dynamics of an impact system of two concentric hollow cylinders with a clearance. Shan et al. [7] studied an electronic device dropping at an inclination angle to the floor. Results of numerical simulation indicated that subsequent impacts might be larger than the initial impact in some situations. Liu et al [8] studied the effect of contact model on elastic-plastic sub-impacts.

According to experimental results, Stoianovici and Hurmuzlu [1] assumed that the vibrational motion of bars during the collision process increased the possibility of occurrence of the sub-impacts. Recently, Langley [9] applied random vibration theory to study the characteristics of impact force and effect of impact location on impact force in randomly vibrating elastic systems. Results show that sub-impacts can occur under certain conditions.

In the present investigation, a dynamic substructure technique for elastic-plastic impact [10]-[11] is applied to simulate a rigid hemispherical-head block transversely impacting on a both-side simply supported beam at five different locations. The effect of impact location on sub-impacts is found by computing the time history of impact force and energy exchange.

II. Numerical Model

A. Problem Description

Consider a rigid hemispherical-head block impacting on a uniform beam clamped at both sides, as seen in Fig. 1. The beam is of length L, thickness h, width b, mass density ρ, Young's modulus E and yield stress Y. The block is of mass m, hemisphere radius R and initial velocity v_0. The beam is simplified as Bernoulli-Euler beam. A linear elastic-perfectly plastic constitutive relation is adopted and small displacements are assumed, i.e., geometrical nonlinearity is neglected.

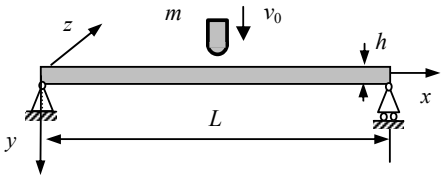

Fig. 1 A rigid hemispherical-head block transversely impacts on a beam that is clamped at both sides

B. Theoretical Basis

The beam is discretized into d substructures with n elements in each substructure, as seen in Fig. 2. Take the ith substructure (i=1, 2, … , d), for example, the governing equation in incremental form for elastic-plastic dynamics can be written as

T. F. Jin is with the Department of Mechanics and Engineering Science, Nanjing University of Science and Technology, Nanjing, 210094, People's Republic of China (e-mail: jintengfei20@163.com).
X. C. Yin is with the Department of Mechanics and Engineering Science, Nanjing University of Science and Technology, Nanjing, 210094, People's Republic of China (e-mail: yinxiaochun2000@aliyun.com).
P. B. Qian is with the Jiangsu IntelliSense Technology Co., Ltd., Nanjing, 210094, People's Republic of China (e-mail: qian852002@yahoo.com.cn).

$$\boldsymbol{M}^{(i)}\Delta\ddot{\boldsymbol{a}}^{(i)} + {}^{\tau}\boldsymbol{K}_{ep}^{(i)}\Delta\boldsymbol{a}^{(i)} = {}^{t+\Delta t}\boldsymbol{Q}_l^{(i)} - {}^{t}\boldsymbol{Q}_i^{(i)}\ (t \le \tau \le t+\Delta t) \qquad (1)$$

where $\Delta\boldsymbol{a}^{(i)}$, $\Delta\ddot{\boldsymbol{a}}^{(i)}$, $\boldsymbol{M}^{(i)}$ and ${}^{\tau}\boldsymbol{K}_{ep}^{(i)}$ are the vector of incremental displacement, vector of incremental acceleration, mass matrix and stiffness matrix, respectively. ${}^{t+\Delta t}\boldsymbol{Q}_l^{(i)}$ is the external force matrix at time $t+\Delta t$ and ${}^{t}\boldsymbol{Q}_l^{(s)}$ the internal force matrix at time t.

Using the synthetic substructure technique of fixed-interface mode, the vector of incremental displacement $\Delta\boldsymbol{a}^{(i)}$ can be expressed by the modal coordinate $\Delta\boldsymbol{p}^{(i)}$ to which the modes $\boldsymbol{\Phi}^{(i)}$ are corresponding,

$$\Delta\boldsymbol{a}^{(i)} = \boldsymbol{\Phi}^{(i)}\Delta\boldsymbol{p}^{(i)} = \left[\boldsymbol{\Phi}_N^{(i)} \quad \boldsymbol{\Phi}_C^{(i)}\right]\Delta\boldsymbol{p}^{(i)} \qquad (2)$$

where $\boldsymbol{\Phi}_N^{(i)}$ and $\boldsymbol{\Phi}_C^{(i)}$ are the fixed-interface normal modal matrix and constraint modal matrix, respectively. The existence of the fixed-interface normal modes and the convergence of the truncation of the fixed-interface normal modes were proved by Qian et al. [10].

The modal set $\boldsymbol{\Phi}$ of the beam can be obtained by assembling the modes of all substructures. The generalized modal mass matrix $\bar{\boldsymbol{M}}$ and stiffness matrix ${}^{\tau}\bar{\boldsymbol{K}}$ of the beam can be obtained from

$$\bar{\boldsymbol{M}} = \boldsymbol{\Phi}^{\mathrm{T}}\boldsymbol{M}\boldsymbol{\Phi},\ {}^{\tau}\bar{\boldsymbol{K}} = \boldsymbol{\Phi}^{\mathrm{T}\,\tau}\boldsymbol{K}_{ep}\boldsymbol{\Phi} \qquad (3)$$

where $\boldsymbol{M}$ and ${}^{\tau}\boldsymbol{K}_{ep}$ are generalized mass matrix and stiffness matrix.

The dynamics equation of the beam in modal space can be written as

$$\bar{\boldsymbol{M}}\Delta\ddot{\boldsymbol{p}}(t) + {}^{\tau}\bar{\boldsymbol{K}}\Delta\boldsymbol{p}(t) = \boldsymbol{\Phi}^{\mathrm{T}\,t+\Delta t}\boldsymbol{Q}_l - \boldsymbol{\Phi}^{\mathrm{T}t}\boldsymbol{Q}_i\ (t \le \tau \le t+\Delta t) \qquad (4)$$

where ${}^{t+\Delta t}\boldsymbol{Q}_l$ is the external force matrix at time $t+\Delta t$, and ${}^{t}\boldsymbol{Q}_i$ the internal force matrix at time t.

The dynamic equation of rigid block is

$$m\Delta\ddot{a}^{l} = -{}^{t+\Delta t}F + m\,{}^{t}\ddot{a}^{l} \qquad (5)$$

where ${}^{t+\Delta t}F$ is the contact-impact force exerted on contact point at time $t+\Delta t$, and $\ddot{a}^{l}$ the acceleration of rigid block at time t.

An elastic-plastic local contact model of the block into the beam, UC model [8], is shown in Fig. 3. The contact force F associate to indentation δ is calculated by the local contact model.

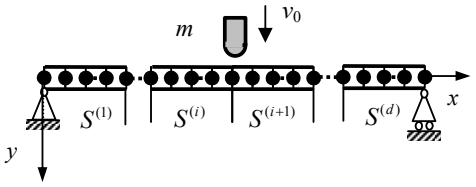

Fig. 2 Substructure model of the beam

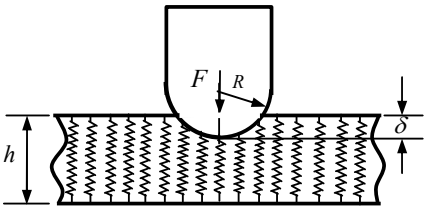

Fig. 3 Elastic-plastic contact model

III. Results and Discussion

At the numerical simulation of sub-impacts of the block against the beam, the beam size is chosen as L=0.78m, h=0.06m, b=0.027m. The beam material properties are of ρ=7800kg/m^3, E=210GPa and Y=235MPa. The block mass is 2.05kg, and the hemispherical-head is R=0.045m. The initial impact velocity of the block is v_0=2.70m/s. The number of substructures is d=40, and the number of elements in each substructure is n=3. Two normal vibration modes are used to represent the deformation field in the beam.

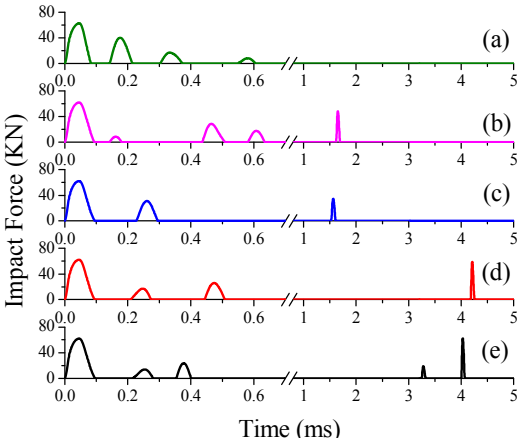

Fig. 4 Time history of sub-impact force for five impact locations (a) impact at 10% of the beam length measured from the boundary (b) 20% (c) 30% (d) 40% (e) 50%

The effect of impact location on time history of sub-impact force is shown in Fig. 4. The time histories of sub-impact force are simulated numerically for the five impact locations at 10%, 20%, 30%, 40% and 50% of the beam length measured from the boundary. For the five impact locations, the sub-impacts end up at 0.6ms, 1.7ms, 1.6ms, 4.3ms, 4.1ms, respectively. If the impact duration is defined from the beginning of the sub-impact to the end of the last sub-impact, it illustrates that the impact

location has a significant effect on the impact duration and the impact duration increases in general as impact location is farer from the boundary. The reason might be the increase of the beam flexibility at impact location without considering the local contact deformation.

However, the duration and magnitude of the first sub-impact force change little with the impact location. The duration has slight increase as the impact location closes to the middle of the beam. It's clear that the impact location has little influence on the first sub-impact. It is perhaps that the global deformation response of the beam has not been excited by the first sub-impact of very short duration, for example, 95 microseconds as shown in Fig. 4 (e).

The effect of impact location on the kinetic energy of the block (as percentages of the total kinetic energy at the onset of impact) is shown in Fig. 5. The time histories of the kinetic energy of the block are simulated numerically for the five impact locations at 10%, 20%, 30%, 40% and 50% of the beam length measured from the boundary. The majority of the kinetic energy is absorbed by the beam. The remained kinetic energy of the block flew off is 1.1%, 13.5%, 3.1%, 13.8%, 19.2% of the initial impact kinetic energy, respectively. In general, the larger the beam flexibility at impact location is, the higher rebounded velocity of the block is. However, there is an exception for the impact location at 30% of the beam length measured from the boundary. Hence, the energy exchange between the beam and the block is affected, sometimes sensitively, by impact location.

In Fig. 5 (a), the energy of the block decreases drastically in the first two sub-impacts, and the beam absorbs 98.6% of the initial impact kinetic energy. As shown in the small plot in Fig. 5 (a), during the third sub-impact, the kinetic energy of the block loses firstly, and then recovers a little. During the fourth sub-impact, the block absorbs continuously the energy from the beam.

In Fig. 5 (b), the energy of the block decreases steadily in the first four sub-impacts, and the beam absorbs 99.9% of the initial impact kinetic energy, but during the fifth sub-impact, the block absorbs continuously the energy from the beam.

In Fig. 5 (c), the energy of the block decreases drastically in the first two sub-impacts, and the beam absorbs 98.5% of the initial impact kinetic energy. As shown in the small plot in Fig. 5 (c), during the third sub-impact, the kinetic energy of the block loses firstly, and then recovers.

In Fig. 5 (d), the energy of the block decreases steadily in the first three sub-impacts, and the beam absorbs 99.8% of the initial impact kinetic energy, but during the fourth sub-impact, the block absorbs continuously the energy from the beam.

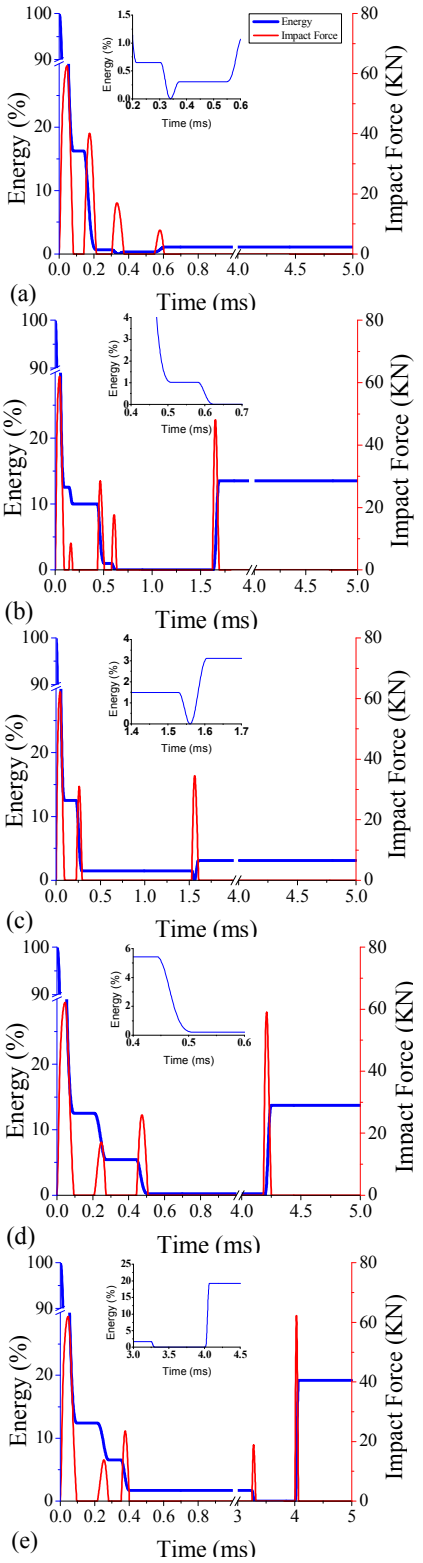

Fig. 5 Time history of sub-impact force and block kinetic energy for five impact locations (a) impact at 10% of the beam length measured from the boundary (b) 20% (c) 30% (d) 40% (e) 50%

In Fig. 5 (e), the energy of the block decreases steadily in the first four sub-impacts, and the beam absorbs 99.9% of the initial impact kinetic energy, but during the fifth sub-impact, the block absorbs continuously the energy from the beam.

The above discuss illustrates that there are three types of energy exchange in the process of single sub-impact between the beam and the block. The first type is the beam absorbing energy from the block. It takes place during the first several sub-impacts. The second type is the beam absorbing firstly energy from the block, and then releasing its energy to the block. The third type is the block absorbing energy from the beam. It's found that the block does not merely rebound during the last sub-impact, and the rebound of the block might take place before the last sub-impact.

IV. Conclusion

The present study simulates a rigid block transversely impacting a both-side simply supported beam at five different locations, and analyzed the variations of sub-impact force and the block kinetic energy. The results show clearly that the impact location has a significant effect on impact duration and energy exchange, but the duration and magnitude of the first sub-impact force change little with the impact location. There are three types of energy exchange in the process of single sub-impact. It's found that the block rebound not only during the last sub-impact, but also before the last sub-impact.

Acknowledgment

This paper is supported by Nanjing University of Science and Technology, and Provincial Natural Science Research Project of Anhui Colleges (KJ2013Z021).

References

[1] D. Stoianovici and Y. Hurmuzlu, "A critical study of the applicability of rigid-body collision theory," *Journal of Applied Mechanics,* vol. 63, pp. 307-316, 1996.

[2] H. L. Mason, *Impact of beams.* vol. 58: Transactions of the American Society of Mechanical Engineers, 1935, pp. 55-61.

[3] W. Goldsmith, *Impact: the theory and physical behaviour of colliding solids.* Dover Pubns, 1960.

[4] X. C. Yin, "Multiple impacts of two concentric hollow cylinders with zero clearance," *International Journal of Solids and Structures,* vol. 34, pp. 4597-4616, 1997.

[5] P. R. Marur, "Charpy specimen--a simply supported beam or a constrained free-free beam?," *Engineering Fracture Mechanics,* vol. 61, pp. 369-386, 1998.

[6] X. C. Yin and L. G. Wang, "The effect of multiple impacts on the dynamics of an impact system," *Journal of Sound and Vibration,* vol. 228, pp. 995-1015, 1999.

[7] H. Shan, J. Su, F. Badiu, J. Zhu, and L. Xu, "Modeling and simulation of multiple impacts of falling rigid bodies," *Mathematical and Computer Modelling,* vol. 43, pp. 592-611, 2006.

[8] Z. H. Liu, X. C. Yin, and L. Tang, "Comparison of simulation results of local contact deformable models on multiple elastic-plastic impacts of simply supported beam," *Journal of Nanjing University of Science and Technology (Natural Science),* vol. 6, pp. 739-744, 2009.

[9] R. S. Langley, "The analysis of impact forces in randomly vibrating elastic systems," *Journal of Sound and Vibration,* 2012.

[10] P. B. Qian, X. C. Yin, Y. N. Shen, and J. Yang, "Dynamic substructure method for propagation of elastic-plastic wave induced by impact," *Chinese Journal of Theoretical and Applied Mechanics,* vol. 44, pp. 184-188, 2012.

[11] P. B. Qian, X. C. Yin, Y. N. Shen, J. Yang, and D. P. Kong, "Dynamic substructure technique for elastic-plastic impact responses of simply supported beam," *Journal of Nanjing University of Science and Technology,* vol. 36, pp. 176-181, 2012.